CHEMBIOCHEM

Supporting Information

A Fluorimetric Readout Reporting the Kinetics of Nucleotide-Induced Human Ribonucleotide Reductase Oligomerization

Yuan Fu,[a] Hong-Yu Lin,[a] Somsinee Wisitpitthaya,[a] William A. Blessing,[a] and Yimon Aye*[a, b]

cbic_201402368_sm_miscellaneous_information.pdf

CONTENTS

General Materials and Methods. BL21-CodonPlus(DE3)-RIL competent cells were from Stratagene. Calf intestine alkaline phosphatase was from NEB. NH_4^+ salt of [5-^{3}H]-CDP was from Vitrax. ClF was from Selleckchem. ClFDP and ClFTP were synthesized as previously reported (*1*). 5-Iodoacetamido-fluorescein (5-IAF), tetramethylrhodamine-5-iodoacetamide-dihydroiodide (5-TMRIA), and dATP were from Invitrogen. Liquid scintillation counting cocktail (Emulsifier-Safe) was from Perkin Elmer. All primers for were from IDT. Fusion HotStartII polymerase was from Thermo. Complete EDTA-free protease inhibitor tablets, DNase I and all the restriction enzymes were from NEB. TALON metal affinity resin was from Clontech. Sephadex G-25 resin, PD-10 Sephadex G-25M mini desalting columns and the gel filtration molecular weight standards were from GE Healthcare. Additional gel filtration standards, β-amylase (A8781) and alchohol dehydrogenase (A8656), were from Sigma, and bovine serum albumin was from BioRad (500-0206). Ultrafiltration Membrane Amicon Ultra centrifugal devices were from Millipore. ATP was from Acros Organics. NADPH was from MP Biomedicals. Dithiothreitol (DTT), streptomycin sulfate and isopropyl β-D-1-thiogalactopyranoside (IPTG) were from Gold Biotechnology. All other chemicals were from Sigma. His-tagged *E. coli* thioredoxin reductase (His_6-TrxR) (*2*), and human RNR subunits: His_6-α, -D57N-α and -β, were isolated, and the metallocofactor was reconstituted (*1, 3*), as previously described. A pET28a vector encoding *E. coli* thioredoxin (Trx) gene was generated from the plasmid A307 pTrxA bearing wild type *E. coli* Trx gene (a kind gift of Professor Charles Richardson's laboratory, Harvard Medical School, MA) (*4*). His_6-Trx was subsequently expressed in *E. coli* and purified to homogeneity by TALON-affinity chromatography. The activity of the isolated His_6-Trx was 22 ± 3 $nmolmin^{-1}mg^{-1}$

based on the DTNB-coupled spectrophotometric assay(*5*). Protein concentrations were determined using $\varepsilon_{280nm}/M^{-1}cm^{-1}$: 119,160 and 45,900 for α or D57N-α, and β (calculated from the amino acid sequence using the ProtParam tool (http://web.expasy.org/protparam/). All concentrations reported are for monomers. The extinction coefficients of IAF and TAMRIA were $\varepsilon_{492nm}/M^{-1}cm^{-1}$ 81,000 and $\varepsilon_{548nm}/M^{-1}cm^{-1}$ 78,000, respectively (source: Genaxxon Bioscience, Germany), and were assumed unaffected by protein conjugation. All experiments with the fluorescently labeled proteins were performed in dark at the indicated temperature. Curve fitting was performed using Kaleida graph (version 4.1.2) and Berkeley Madonna (version 8.3.18).

SUPPORTING METHODS

Fluorescent Dye Labeling of His_6-α and –D57N-α (Figure 2A and S6A). The labeling reaction in a final volume of 250 μL in final concentrations contained recombinantly purified 10 μM hRNR His_6-α or –D57N-α (*1*), 30 μM 5-IAF or 5-TMRIA, 15 mM $MgCl_2$, 1 mM DTT in 50 mM Hepes (pH=7.6). Presence of DTT was necessary for α stability. The mixture was incubated in the dark for 20 min at room temperature by using a rotatory mixer. The reaction mixture was desalted on a PD-10 Sephadex G-25M column (GE Healthcare) that had been pre-equilibrated with 50 mM Hepes (pH=7.6), 15 mM $MgCl_2$ and 5 mM DTT. Fractions containing labeled proteins were pooled and the final concentration was adjusted to 1 μM with the same buffer. Control experiment was performed under identical conditions except that DMSO (0.03 % v/v) replaced the fluorescent dyes. Labeled proteins were immediately carried onto subsequent experiments.

Quantitation of Labeling Efficiency (Table S1, Figure 2B and S6B). The labeled protein was concentrated to 3–4 μM by Amicon Ultra 0.5 ml Filters (30 kDa MWCO, Millipore) and the absorption spectra of the labeled protein were recorded in the wavelength range 240–700 nm at room temperature using a Nanodrop ND-1000 spectrophotometer. The labeling efficiency was calculated as follow:

$$\text{Labeling efficiency for Fluorescein} = \frac{\frac{OD496}{\varepsilon_{Fl,496}}}{\frac{OD280 - OD496 \times \frac{\varepsilon_{Fl,280}}{\varepsilon_{Fl,496}}}{\varepsilon_{a,280}}}$$

$$\text{Labeling efficiency for TAMRA} = \frac{\frac{OD553}{\varepsilon_{TMR,553}}}{\frac{OD280 - OD553 \times \frac{\varepsilon_{TMR,280}}{\varepsilon_{TMR,553}}}{\varepsilon_{a,280}}}$$

where OD_{496}, OD_{280} and OD_{593} stand for absorbance at 496 nm, 280 nm and 553 nm respectively. $\varepsilon_{Fl,496}$ and $\varepsilon_{Fl,280}$ are the extinction coefficients of fluorescein at 496 nm and 280 nm. $\varepsilon_{TMR,553}$ and $\varepsilon_{TMR,280}$ are the extinction coefficients of tetramethylrhodamine at 553 nm and 280 nm. $\varepsilon_{a,280}$ is the extinction coefficient of hRNR-α at 280 nm.

LC-MS/MS Determination of Modified Sites (Figure S1). The labeled α was mixed with reducing Laemmli buffer and was electrophoresed through a Tris-Cl gel. The protein was visualized with the Coomassie Brilliant Blue R-250 and the bands representing α were excised. After washing and dehydrating the gel pieces, the proteins were reduced with 10 mM DTT in 100 mM NH_4HCO_3 solution for 45 min at 56 ºC and alkylated with 55 mM iodoacetamide in 100 mM NH_4HCO_3 in dark for 30–60 min. The gel pieces were

rehydrated in 6 μg/mL solution of trypsin in 50 mM NH_4HCO_3 at 30 ºC overnight. Peptides were extracted sequentially with 1% formic acid, 50% acetonitrile containing 5% formic acid and 90% acetonitrile containing 5% formic acid. All supernatants were combined and dried under vacuum. Peptides were resuspended and subjected to LC-MS/MS analysis. Data analysis and processing were performed at the Proteomics and Mass Spectrometry, Cornell University Institute of Biotechnology.

Analytical Gel Filtration (Figure 2C and S2). Gel filtration was performed on a Superdex 200 10/300 column (GE Healthcare) using a Shimadzu Prominence SIL-20ACHT HPLC. The incubation mixture contained 15 mM $MgCl_2$, 3 μM α or D57N-α or the labeled analogs, 5 mM DTT, ± 1 mM dATP or ± 15 μM ClFD(T)P in 50 mM Hepes (pH 7.6). Prior to injection, the reaction mixture was incubated at 37 ºC for 2 min and filtered through 0.22 μm syringe filters (Millex low protein binding PVDF membrane, Millipore). 100 μL of reaction mixture was injected onto the column that had been preequilibrated with the running buffer [15 mM $MgCl_2$, 150 mM NaCl, and ± 20 μM dATP in 50 mM Hepes (pH 7.6)] at room temperature. The flow rate was 0.5 mL/min. Absorbance was monitored at 260, 280 and either 495 (for fluorescein) or 555 nm (for tetramethylrhodamine). Molecular mass standards (GE Healthcare): ovalbumin, 44 kDa; conalbumin, 75 kDa; aldolase, 158 kDa; ferritin, 440 kDa; thyroglobulin, 669 kDa, were run under identical conditions at the end of each run. Additional standards used were β-amylase (tetramer, 200 kDa, Sigma A8781), alcohol dehydrogenase (tetramer, 150 kDa, Sigma A8656), and bovine serum albumin (monomer, 66 kDa, BioRad 500-0206).

Activity of Labeled Proteins (Figure S3A). α-subunit-specific radioactive assays for α and D57N-α (or the labeled analogs) were performed as previously described (*1*). Briefly, 0.5 μM α, 3.5 μM β, 0.5 mM [5-^{3}H]-CDP (21,500 cpm/nmol), 3 mM ATP, 15 mM $MgCl_2$, 100 μM *E. coli* His_6-Trx, 1.0 μM *E. coli* His_6-TrxR, and 2 mM NADPH were mixed in a total volume of 135 μL in 50 mM Hepes buffer (pH 7.6) at 37 ºC. The reaction was initiated by addition of substrate CDP. At 0.7, 1.3, 2.2 and 3.0 min time points post initiation, 30 μL aliquots were removed and quenched with 30 μL 2% $HClO_4$ and neutralized with 30 μL 0.4 M NaOH. Dephosphorylation, isolation of [5-^{3}H]-dCDP and liquid scintiallation counting were performed as previously described (*6*).

Steady-State Fluorescence Assays (Figure 3, S3B, S4, S5 and S9A). Steady-state fluorescence measurements were performed on a Varian Cary Eclipse spectrofluorimeter. The excitation wavelength was 480 nm. The emission spectra were recorded in the wavelength range 505 to 620 nm. The excitation and emission slit width were 20 nm and 10 nm, respectively. Unless otherwise stated, 188 nM F- and T-α (or the D57N-variants) in indicated ratios, 15 mM $MgCl_2$, 5 mM DTT and 50 mM Hepes (pH=7.6) in a total volume of 220 μL was prepared in a 3 mm × 3 mm path length quartz fluorescence microcuvette at room temperature. α-oligomerization was induced by a minimal volume of nucleotide inducer (100 μM final concentration unless otherwise stated). The emission spectra of oligomeric assembly were recorded after incubation for 5 min. In control experiments (Figure S4), 50 mM Hepes (pH=7.6) buffer or unlabeled α replaced either the inducer nucleotide, F- or T-α as indicated. In titration experiments (Figure 2F), dATP-promoted α hexamerization curves were obtained by incubating 0.188 μM of F-

and T-α in indicated ratios in 15 mM $MgCl_2$, 5 mM DTT and 50 mM Hepes (pH=7.6) in the presence of increasing concentration of dATP/ClFD(T)P at room temperature. In subunit exchange experiment (Figure S10), 110 μL solution containing 2 μM unlabeled D57N-α dimers in 200 μM dATP was rapidly mixed with 110 μL solution containing 0.375 μM labeled D57N-α dimers (i.e., 1:1 F-:T-D57N-α in 200 μM dATP). The time course of fluorescence recovery was subsequently monitored at room temperature.

Stopped-Flow Fluorescence Measurements (Figure 4, 5C, 6A-B, S7, S8, S9B and S11A). Stopped-flow fluorescence measurements were performed on a SF-2004 KinTek stopped-flow spectrophotometer. In the experiments with dATP alone, syringe A contained 1:5 mixture of F-α and T-α (188–658 nM) in 50 mM Hepes pH=7.6, 15 mM $MgCl_2$ and 5 mM DTT. Syringe B contained either no or indicated concentrations (100–200 μM) of dATP in 50 mM Hepes pH=7.6, 15 mM $MgCl_2$ and 5 mM DTT. In the experiments for monitoring $\alpha_2 \rightarrow \alpha_6$ transition, syringe A additionally contained 0.1 mM dGTP. The reaction was maintained at 25 ºC with a circulating water bath. The contents of syringe A and syringe B were rapidly mixed in a 1:1 ratio. Total fluorescence at wavelengths > 505 nm was monitored using a PMT detector with a long-pass filter, using an excitation wavelength of 480 nm and entry slit width of 0.76 mm. The fluorescence scans were collected in 10s or 320s data files and each file is consisted of 1000 data points. The dead time of the instrument was 1 ms. No significant photobleaching of the fluorophores was observed during the course of the stopped-flow experiments (Figure S7A). At least nine measurements were obtained for each sample to give one averaged kinetic trace.

Derivation of Eq 1 (second-order dimerization rate-law):
For the dimerization event: $\alpha + \alpha \rightarrow \alpha^2$, the rate is $k[\alpha]^2$

where k is a rate constant and $[\alpha]$ is the concentration of α monomer at time t.

The time course of the α monomer is

$$d[\alpha]/dt = -2k[\alpha]^2.$$

Integration results in $$[\alpha] = [\alpha]_0 / (1 + 2[\alpha]_0 kt) \qquad \text{(Eq S1)}$$

where $[\alpha]_0$ is the monomer concentration at time zero.

The measured fluorescence intensity at time t, i.e., $I(t)$, is related to the concentration of monomers: $[\alpha]$, and dimers: $([\alpha] - [\alpha]_0)/2$, at a given time, by the following equation:

$$I(t) = p\,[\alpha] + q\,([\alpha]_0 - [\alpha]) \qquad \text{(Eq S2)}$$

where p and q are constants.

From Eq S2,

$$I_0 = p\,[\alpha]_0 \text{ at time zero and} \qquad \text{(Eq S3)}$$

$$I_\infty = q\,[\alpha]_0 \text{ at an infinite time.} \qquad \text{(Eq S4)}$$

Substituting p and q of Eq S2 by using Eq S3 and S4 results in:

$$I(t) = \left[\left(I_0 - I_\infty\right)\frac{[\alpha]}{[\alpha]_0}\right] + I_\infty \qquad \text{(Eq S5)}$$

Substituting $[\alpha]/[\alpha]_0$ in Eq S5 with Eq S1 gives:

$$I(t) = \frac{I_0 - I_\infty}{1 + 2[\alpha]_0 kt} + I_\infty \qquad \text{(Eq 1)}$$

Eq 1 can be simply viewed as $y = \frac{a}{1 + b\,t} + c$ where a, b and c are constants.

This equation was used to fit the averaged fluorescence traces shown in Figure S7 and Figure S9B by using Kaleida graph (version 4.1.2).

Derivation of Eq 2.4:

The two-step kinetics of dATP-promoted wt-α hexamerization were modeled by the transformation: $\alpha \rightarrow \alpha^* \rightarrow (\alpha^*)_2$, in which the second step is rate-determining. α* is the intermediate formed during the fast phase proposed to be conformationally altered α, and $(\alpha^*)_2$ is the dimer that once formed, proceeds to hexamerize at a rate faster than the rate-determining dimerization. Because steps subsequent to the rate-determining $(\alpha^*)_2$ formation were not revealed by the observed kinetic trace, exclusion of $(\alpha^*)_6$ did not affect the following kinetic derivation. Note however that $(\alpha^*)_2$ did not accumulate but was rapidly converted to $(\alpha^*)_6$.

The time course of each species can be presented by Eq 2.1–2.3:

$$d[\alpha]/dt = -k_1 [\alpha] \qquad \text{(Eq 2.1)}$$

$$d[\alpha^*]/dt = k_1[\alpha] - 2k_2 [\alpha^*]^2 \qquad \text{(Eq 2.2)}$$

$$d[(\alpha^*)_2]/dt = k_2 [\alpha^*]^2 \qquad \text{(Eq 2.3)}$$

where k_1 and k_2 respectively designate the rate constants for the first and second step.

The measured fluorescence intensity at time t, i.e., $I(t)$, is given by

$$I(t) = p [\alpha] + q [\alpha^*] + r (\alpha^*)_2 \qquad \text{(Eq S6)}$$

where p, q and r are constants, and [α], [α*], and $[(\alpha^*)_2]$ are concentrations of the three species.

At any given time t, $\quad [\alpha] + [\alpha^*] + 2[(\alpha^*)_2] = [\alpha]_0 \qquad$ (Eq S7)

where $[\alpha]_0$ is the initial protein concentration.

Substituting [α] in Eq S6 with Eq S7 yields:

$$I(t) = p [\alpha]_0 - (p - q) [\alpha^*] - (2p - r) [(\alpha^*)_2] \qquad \text{(Eq S8)}$$

Eq S8 can be considered as:

$$I(t) = I_0 - U[\alpha^*] - V[(\alpha^*)_2] \qquad \text{(Eq 2.4)}$$

where I(t) is the total fluorescence intensity at time t. I_0 is the fluorescence intensity at time zero. U and V are constants. The set of equations 2.1–2.4 was used to fit the averaged kinetic trace shown in Figure 3C by using the Berkeley Madonna software (version 8.3.18).

SUPPORTING TABLE

Table S1. Labeling efficiencies of His_6-α and His_6-D57N-α

	+ IAF	+ TMRIA
His_6-α	0.97 ± 0.16	0.88 ± 0.14
His_6-D57N-α	0.87 ± 0.11	0.94 ± 0.25

Shown as number of equivalents per α. Standard deviation was derived from N = 3 and 2 for wt- and D57N-α, respectively. See page 4 (SI) for calculations of labeling efficiency.

Table S2. Rate constants at different wt-α concentrations: from fitting the kinetic traces of dATP-induced wt-α hexamerization to Eq 2.1–2.4

[α] (μM)	k_1 (s^{-1})	k_2 (× 10^4 $M^{-1}s^{-1}$)
0.1	1.4 ± 0.1	7.3 ± 0.4
0.15	1.7 ± 0.7	6.3 ± 0.2
0.2	1.1 ± 0.2	7.9 ± 0.4
0.25	1.2 ± 0.2	6.5 ± 0.3
0.3	1.4 ± 0.2	7.1 ± 0.6
0.35	1.2 ± 0.3	6.3 ± 0.3

SUPPORTING FIGURES

Figure S1

A

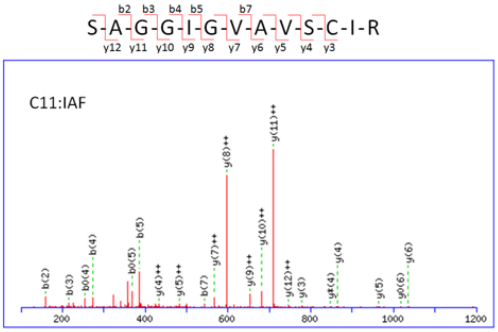

B

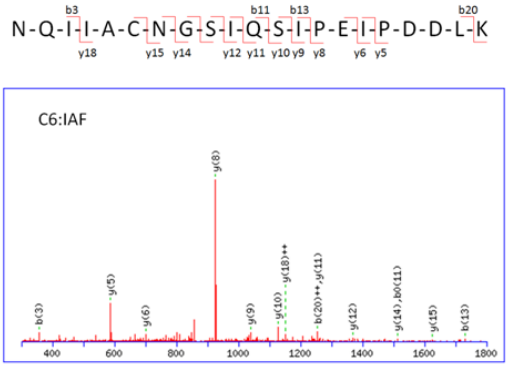

C

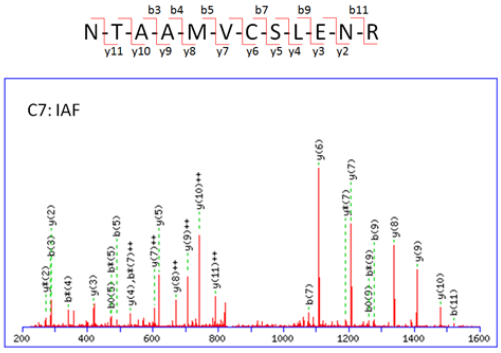

Figure S1. Peptide sequencing data from LC-MS/MS analysis. Representative MS/MS peptide sequencing data for fluorescein-labeled wt-His_6-α. Tryptic peptides in which indicated Cys were alkylated by IAF: (**A**) 244–256 (57, $1.3x10^{-5}$), (**B**) 657–677 (58, $6.1x10^{-6}$), (**C**) 773–784 (55, $1.7x10^{-5}$). Numbers in parentheses indicate peptide score and expectation values, respectively. Only peptides with score > 40 are presented. Protein sequence coverage was 69%. The residue numbers shown for the peptides correspond to untagged-α.

Figure S2

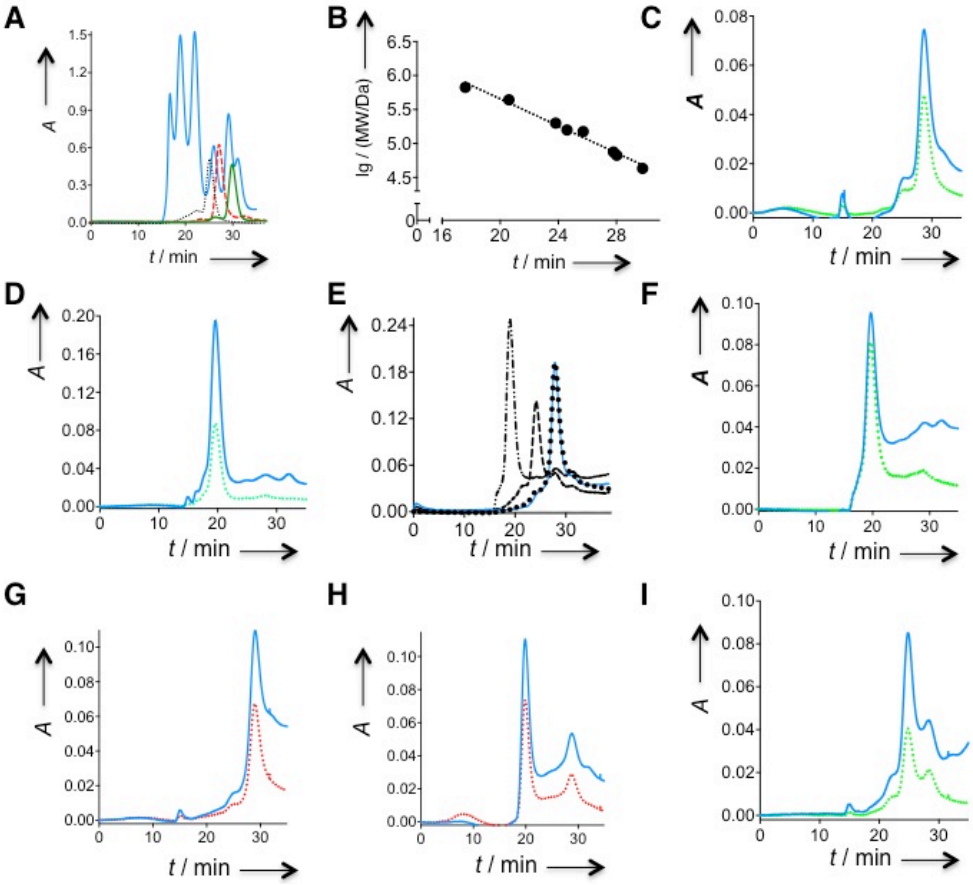

Figure S2. Representative gel filtration elution profiles of labeled proteins. In C, D and F—I, —, … and … designate A280, A495 and A555 traces, respectively. (**A**) — Indicates elution profile of a mixture of GE Healthcare MW standards: thyroglobulin (669 kDa, 17.6 min); ferritin (440 kDa, 20.6 min); aldolase (158 kDa, 24.6 min); conalbumin (75 kDa, 27.8 min); ovalbumin (44 kDa, 29.8 min). Additional standards: β-amylase (200 kDa, 23.8 min, …); alcohol dehydrogenase (150 kDa, 25.7 min, **---**); and BSA (66 kDa, 28.0 min, **—**) were independently run. (**B**) MW standard curve. (**C**) F-α alone. (**D**) F-α with 20 μM dATP in the running buffer. Figure 2C is an overlay of (C) and (D). (**E**) Data with unlabeled α: —, …, ---, and -..-.. designate wt-α, D57N-α, either D57N-α or wt-α with 20 μM dATP in the running buffer, respectively. (**F**) F-α pre-treated with 15 μM ClFDP. (**G**) T-α alone. (**H**) T-α in the presence of 20 μM dATP in the running buffer. (**I**) F-D57N-α with 20 μM dATP in the running buffer. N-terminal His_6-tag was present in all cases. Concentration range of α employed in all experiments was 2–5 μM. Retention times: α (92 kDa), 28 min; α_2, 25 min; α_4, 22 min; and α_6, 19 min.

Figure S3

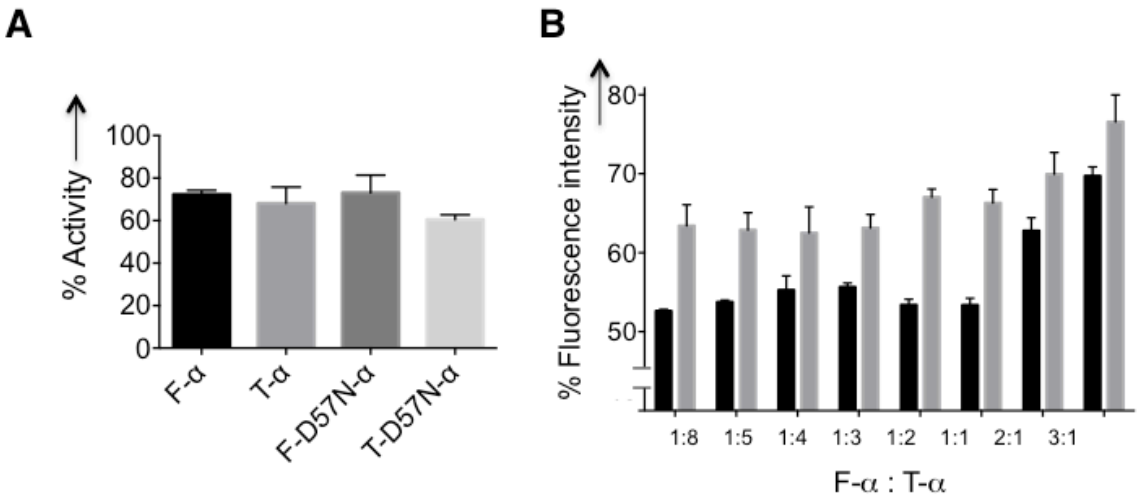

Figure S3. (**A**) Comparison of the α-specific CDP reductase activities of the labeled wt- and D57N-α with respect to unlabeled-α treated under otherwise identical conditions. Specific activities of the recombinant hRNR-α variants were measured as previously reported (*1*). 100% activity corresponds to 570 nmol of dCDP produced per min per mg of His_6-α. (**B**) At the ratios of F:T-α employed in this study, 10 ± 3% difference in fluorescence quenching exists between $\alpha \rightarrow \alpha_2$ and $\alpha \rightarrow \alpha_6$ transitions. % fluorescence intensity refers to the fluorescein intensity at 520 nm within the emission spectra obtained in the presence of 200 μM relative to 0 μM dATP. Black and gray bars correspond to wt- and D57N-α, respectively. S.D. was derived from N = 3 (from independently labeled batches of each protein).

Figure S4

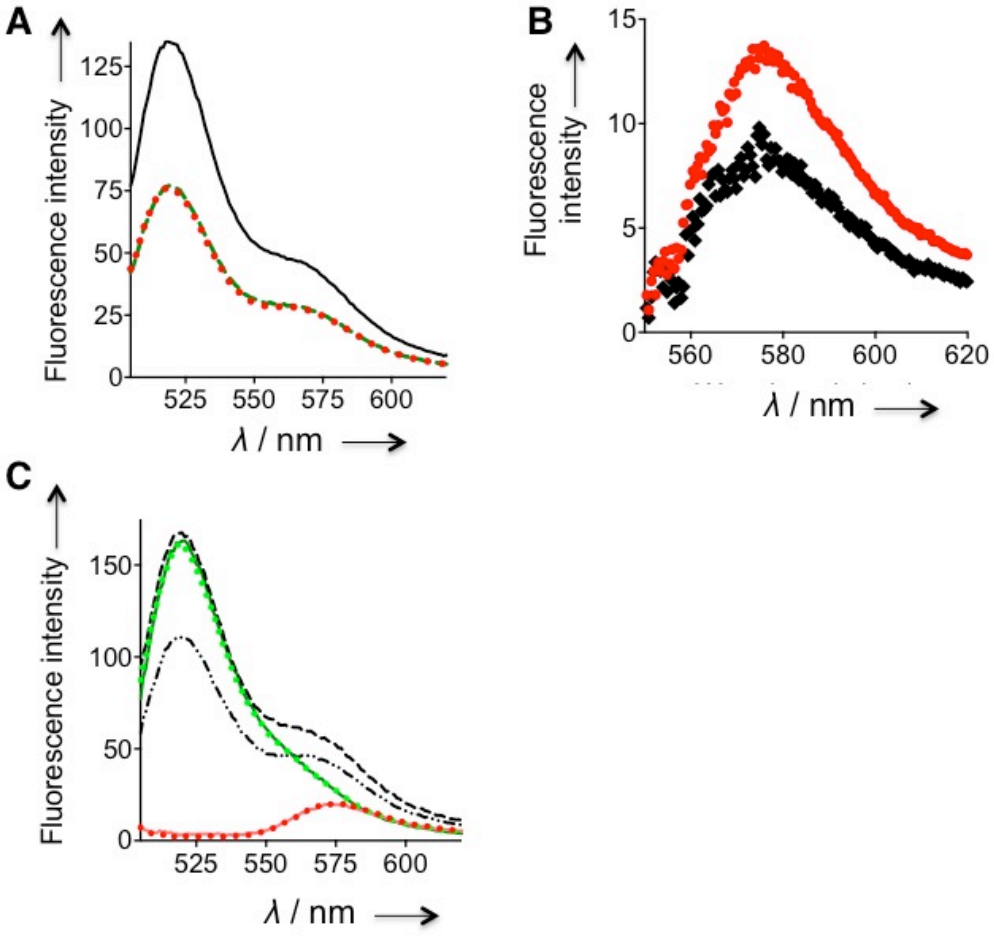

Figure S4. (**A**) Fluorescence emission spectra of 1:5 F-:T-α (0.2 μM) in 1.0 μM ClFD(T)P. —, no drug; ---, ClFDP; …, ClFTP. Also see Figure 3B and S5. (**B**) The rise in T-α-specific emission intensity from 0 (◆) to 200 (●) μM dATP validates the presence of genuine FRET that is coupled with the dATP-induced formation of α_6 state. The two traces were obtained by subtraction of F-α-specific emission spectra (collected from F-α alone samples) from the emission spectra of the samples containing 2:1 F- and T-α in the absence and presence of dATP. The wavelength at the peak maximum observed also lies close to the known λ_{em} for TMR. (**C**) By contrast, there was no drop in fluorescence intensity upon adding 200 μM dATP to either F-α alone or T-α alone samples. F-α (0.2 μM) alone with (—) and without (…) dATP; T-α (0.2 μM) alone with (—) and without (…) dATP; 1:5 F-:T-α (0.2 μM) with (–··–··–) and without (– – –) dATP.

Figure S5

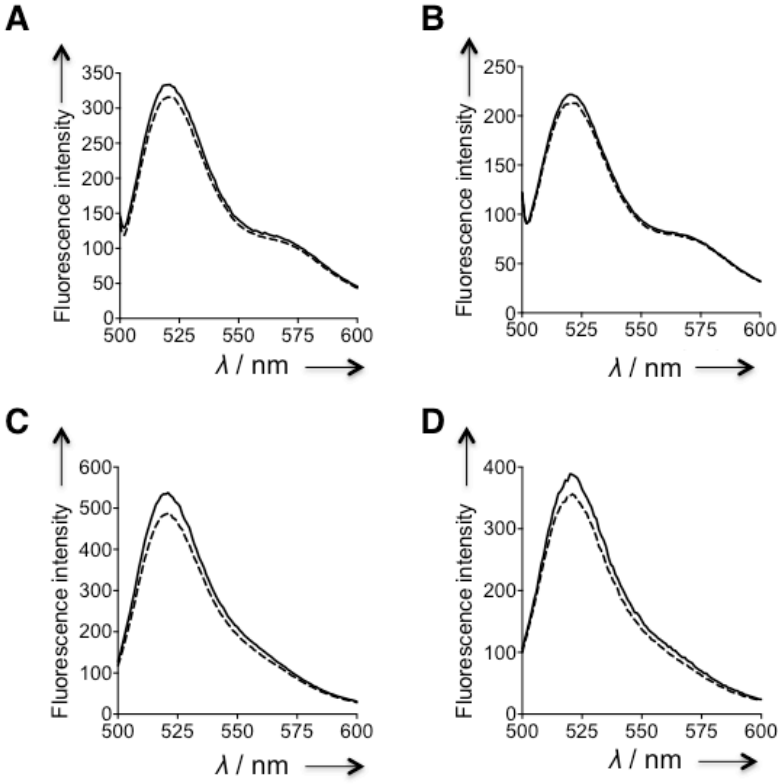

Figure S5. Fluorescence quenching was specific to hexamerization-inducers dATP/ClFD(T)P (A–B) and required interactions between F-α and T-α (C–D). Emission spectra of 1:5 F-α:T-α in the absence (**—**) and presence (**---**) of (**A**) 0.5 mM CDP or (**B**) 10 μM F2CDP (5 equiv). (**C**) Representative emission spectrum of F-α alone in the absence (**—**) and presence (**---**) of 200 μM dATP. (**D**) Representative emission spectrum of 1:5 F-α:unlabeled-α in the absence (**—**) and presence (**---**) of 10 μM ClFDP.

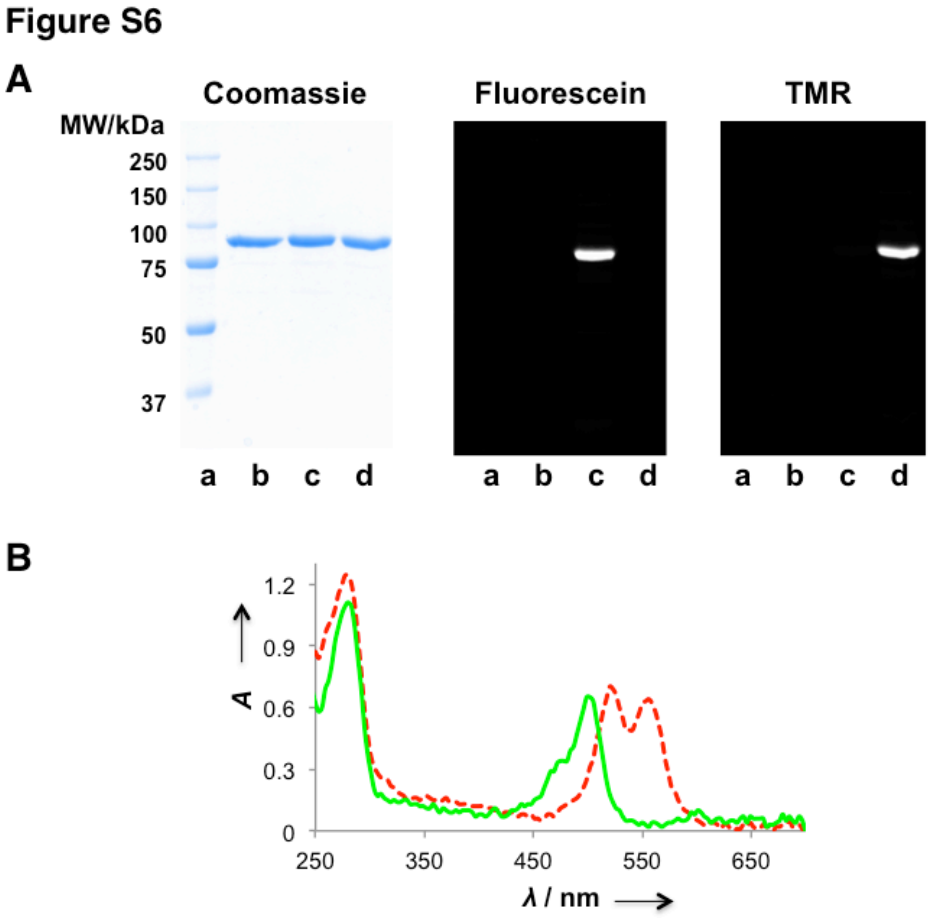

Figure S6. Characterizations of fluorescein (F)- and tretramethylrhodamine (T)-labeled His_6-D57N-α. (**A**) In-gel fluorescence analysis using denaturing SDS-PAGE validates covalent labeling. Lane a, ladder. Lane b, unlabeled D57N-α treated under otherwise identical conditions. Lane c, F-D57N-α. Lane d, T-D57N-α. Fluorophore excitation sources were blue and green epi illumination, respectively, and emission filters were 530/28 and 605/50 nm, respectively, for F and T. (**B**) Absorbance spectra analysis of D57N-α labeling efficiency. Representative data for overlay of absorbance traces for F- (—) and T-D57N-α (---). See also Table S1 and Figure 2A–B.

Figure S7

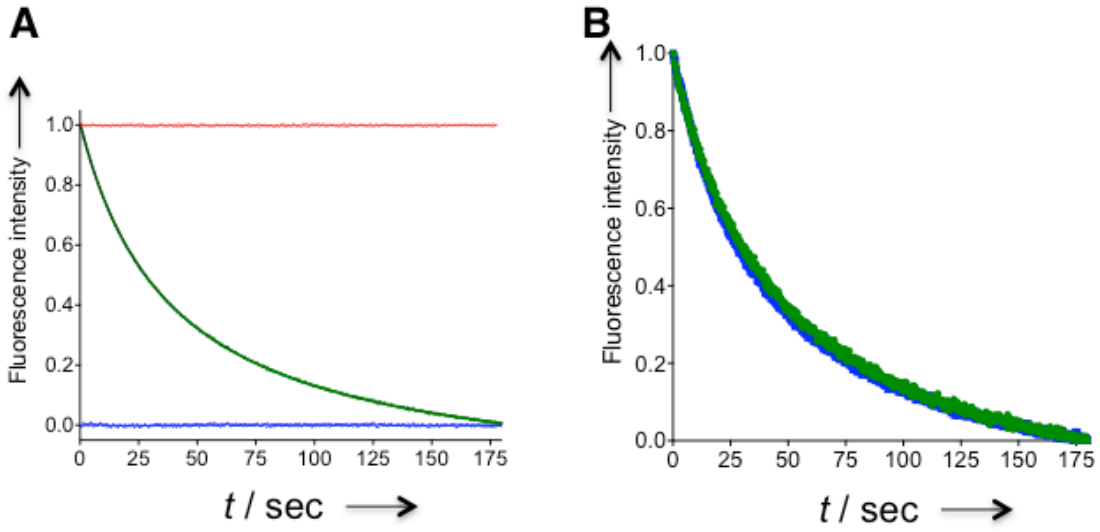

Figure S7. Stopped-flow analysis of the rate of dATP-induced D57N-α dimerization. (**A**) A representative average of ≥9 individual kinetic traces for rapid mixing of 1:5 F-:T-D57N-α (188 nM) and dATP (100 μM) (**green trace**). Fit to the dimerization equation (Eq 1, see main text and SI page 8) is indicated by solid **black** line. Residuals to the fit are shown in **blue**. The red trace was obtained under identical conditions except the second syringe contained buffer only without dATP, suggesting that photobleaching was negligible within this timescale. (**B**) In saturating amounts of dATP, D57N-α dimerization rate is unaffected by [dATP]. **Green** and **blue** traces respectively designate 100 and 200 μM dATP. The data are the average of 9 independent time courses.

Figure S8

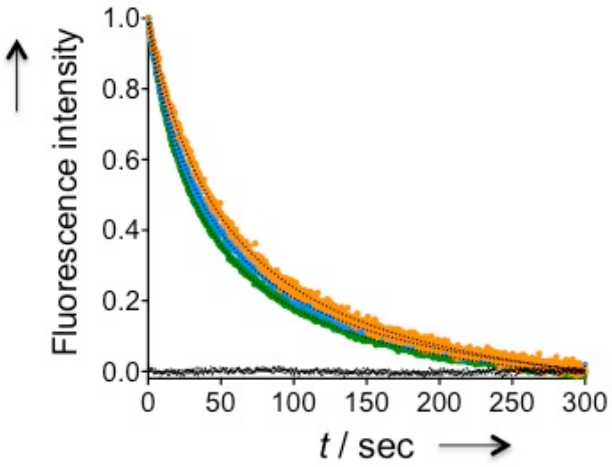

Figure S8. Stopped-flow fluorescence analysis of the effects of low dATP concentrations on the rates of dATP-induced D57N-α dimerization. **Orange**, **Blue**, and **Green** traces designate 20, 33 and 100 μM dATP (final concentrations in the mixing chamber), respectively. Each trace is a representative average of ≥9 individual kinetic traces for a rapid mixing (1:1 v/v) of a mixture of 1:5 F-:T-D57N-α (375 nM), and either 40, 66 or 200 μM dATP. Final total D57N-α concentration was thus 188 nM. The dotted black line within each trace indicates fit to the dimerization equation (Eq 1, see main text and SI page 8). Representative residuals to the fit are shown in the base line for the blue trace (33 μM dATP). The bimolecular rate constants were calculated to be: [(5.0 ± 0.4), (5.9 ± 0.4), and (6.6 ± 0.6)] x 10^4 $M^{-1}s^{-1}$, for 20, 33 and 100 μM dATP respectively. The rate constants derived from these independent runs were of similar magnitudes to that deduced from the data in Figure 4, (5.8 ± 0.2) × 10^4 $M^{-1}s^{-1}$ (Main Text). See also Figure S7.

Figure S9

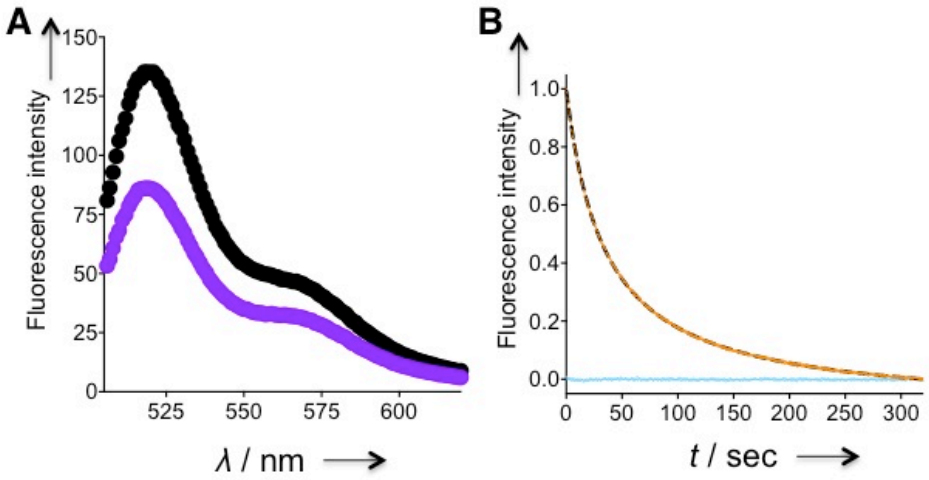

Figure S9. dGTP-induced wt-α dimerization. (**A**) dGTP binding at the S-site induces wt-α dimerization that is coupled with 30–35% (N = 3) quenching of the fluorescein intensity. A representative steady-state fluorescence emission spectrum is shown. (**B**) An averaged (N = 9) stopped-flow kinetic trace (**orange**) for the 0.1 mM dGTP-promoted wt-α dimerization. The **black** dashed line and the **blue** **trace** respectively designate the fit to the dimerization equation (Eq 1, main text, and SI page 8) and residuals.

Figure S10

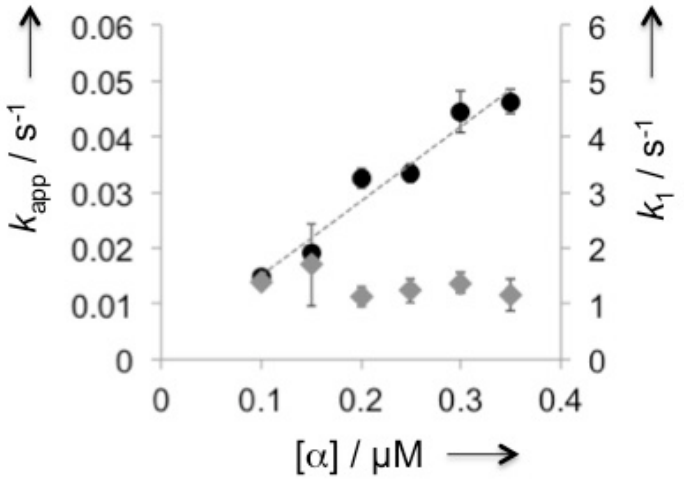

Figure S10. Effects of varying [α] on the two-step kinetics of dATP-induced wt-α hexamerization. k_1 (◆) is the fast step proposed to be linked to the conformational change. k_2 is the rate-determining dimerization. k_{app} (●) is approximated as $2[\alpha]_0 k_2$ in Eq 1 as described in the Main Text page 5. See Table S2 for values of k_1 and k_2 that were derived from fitting the kinetic traces at each [α] to Eq 2.1–2.4 (SI, page 9).

Figure S11

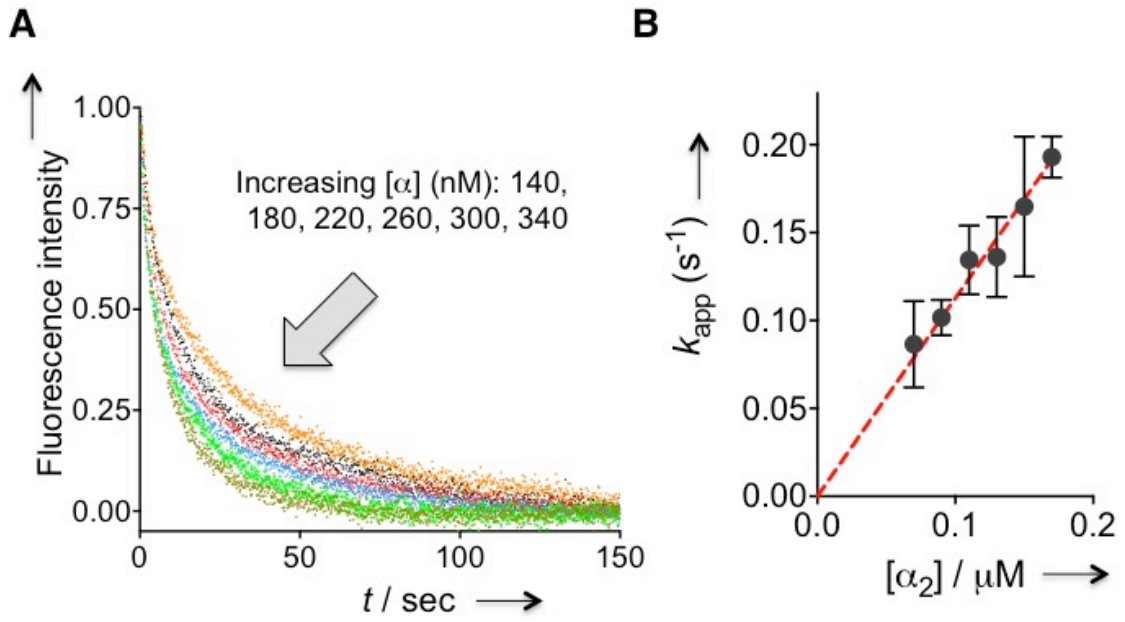

Figure S11. Effects of varying [α] on the rates of $\alpha_2 \rightarrow \alpha_6$ transition. (**A**) Effects of varying [α] (0.14 – 0.34 μM) on the kinetic traces resulting from stopped-flow mixing dATP (200 μM) and wt-α presaturated with dGTP (0.1 mM) at the S site (yellow, dark, red, blue, green, brown traces respectively designate 0.14, 0.18. 0.22, 0.26, 0.30, 0.34 μM α). See also Figure 6A for a representative trace with [α] = 0.2 μM (**B**) The observed k_{app} is linearly dependent on $[\alpha_2]$. $k_{app} = 2[\alpha_2]_0 k$ in Eq 1. See Figure 6B for a representative fit of the kinetic trace (for [α] = 0.2 μM) to Eq 1. Here, Eq 1 is used for modeling $\alpha_2 \rightarrow \alpha_4$ transition, hence protein concentration is presented as dimer concentration.

SUPPORTING REFERENCES

1. Aye, Y., and Stubbe, J. (2011) Clofarabine 5'-di and -triphosphates inhibit human ribonucleotide reductase by altering the quaternary structure of its large subunit, *Proceedings of the National Academy of Sciences of the United States of America 108*, 9815-9820.
2. Fu, Y., Long, M. J., Rigney, M., Parvez, S., Blessing, W. A., and Aye, Y. (2013) Uncoupling of Allosteric and Oligomeric Regulation in a Functional Hybrid Enzyme Constructed from Escherichia coli and Human Ribonucleotide Reductase, *Biochemistry 52*, 7050-7059.
3. Wang, J., Lohman, G. J., and Stubbe, J. (2007) Enhanced subunit interactions with gemcitabine-5'-diphosphate inhibit ribonucleotide reductases, *Proceedings of the National Academy of Sciences of the United States of America 104*, 14324-14329.
4. Johnson, D. E., and Richardson, C. C. (2003) A covalent linkage between the gene 5 DNA polymerase of bacteriophage T7 and Escherichia coli thioredoxin, the processivity factor: fate of thioredoxin during DNA synthesis, *J Biol Chem 278*, 23762-23772.
5. Ellman, G. L. (1959) Tissue sulfhydryl groups, *Archives of Biochemistry and Biophysics 82*, 70-77.
6. Steeper, J. R., and Steuart, C. D. (1970) A rapid assay for CDP reductase activity in mammalian cell extracts, *Analytical biochemistry 34*, 123-130.